INTERNATIONAL JOURNAL FOR NUMERICAL METHODS IN FLUIDS
Int. J. Numer. Meth. Fluids 2003; **42**:1059–1072 (DOI: 10.1002/fld.572)

Linearized and non-linear acoustic/viscous splitting techniques for low Mach number flows

Mohammad Farshchi[1,*,†], Siamak K. Hannani[2] and Mohammad Ebrahimi[2]

[1] *Aerospace Engineering Department, Sharif University of Technology, Tehran, Iran*
[2] *Mechanical Engineering Department, Sharif University of Technology, Tehran, Iran*

SUMMARY

Computation of the acoustic disturbances generated by unsteady low-speed flow fields including vortices and shear layers is considered. The equations governing the generation and propagation of acoustic fluctuations are derived from a two-step acoustic/viscous splitting technique. An optimized high order dispersion–relation–preserving scheme is used for the solution of the acoustic field. The acoustic field generated by a corotating vortex pair is obtained using the above technique. The computed sound field is compared with the existing analytic solution. Results are in good agreement with the analytic solution except near the centre of the vortices where the acoustic pressure becomes singular. The governing equations for acoustic fluctuations are then linearized and solved for the same model problem. The difference between non-linear and linearized solutions falls below the numerical error of the simulation. However, a considerable saving in CPU time usage is achieved in solving the linearized equations. The results indicate that the linearized acoustic/viscous splitting technique for the simulation of acoustic fluctuations generation and propagation by low Mach number flow fields seems to be very promising for three-dimensional problems involving complex geometries. Copyright © 2003 John Wiley & Sons, Ltd.

KEY WORDS: aeroacoustics; low Mach number flow; numerical simulation

1. INTRODUCTION

The generation and propagation of acoustic waves by low-speed flows is of interest for many applications, such as automobile and wind turbine noise. The compressible Navier–Stokes equations describe sound generation and propagation by a general flow field. However, direct numerical simulation of the full compressible equations is prohibitively expensive for low Mach number flows. In fact, direct numerical simulations of the flow induced acoustic disturbances have been restricted to simple model problems to date [1–3]. In an attempt to overcome the difficulties in predicting sound generation and propagation by low Mach number flows, Hardin and Pope [4] proposed an acoustic/viscous splitting technique. In this two-part calculation the viscous flow is first handled by calculating time-dependent incompressible flow, and then the acoustic field is obtained from inviscid equations describing the

*Correspondence to: M. Farshchi, Aerospace Engineering Department, Sharif University of Technology, Azadi Avenue, Tehran, Iran.
†E-mail: farshchi@sharif.edu

Received 28 August 2002
Revised 26 March 2003

differences from the incompressible flow. The same authors used this technique together with a MacCormack predictor–corrector scheme to predict the sound generated by viscous flow over a two-dimensional cavity [5]. Lee and Koo [6] followed this approach to simulate the acoustic field generated by a co-rotating vortex pair. This model problem was also utilized by Ekaterinaris [7] to verify a high order upwind-biased scheme proposed for solving the governing equations in terms of the primitive variables. He later proposed a high order control volume scheme for solving the conservative form of the governing equations [8].

On the other hand, the shortcomings of the classical computational fluid dynamics differencing schemes in aeroacoustics simulations are well documented [9, 10]. To accurately capture the sound wave generation and propagation in a complex flow field higher-order differencing schemes are required. The dispersion–relation–preserving (DRP) schemes have shown their effectiveness in accurately predicting sound wave propagation [10]. In the present study an optimized high order (DRP) scheme together with the acoustic/viscous splitting technique of Hardin and Pope is applied to predict sound generation and propagation by a pair of co-rotating point vortices. This study helps to assess the DRP schemes capabilities in predicting acoustic wave generation. The computed results are compared with existing analytic solutions.

The linearized form of the Hardin–Pope equations is also derived and used to solve this problem. The accuracy of the linearized solution and the resulting savings in computational efforts are discussed.

2. GOVERNING EQUATIONS

There are no truly incompressible fluids in the nature. However, the incompressibility assumption results in a constant density flow field at the limit of low Mach number flows. Fast and efficient numerical techniques have been developed to solve the incompressible Navier–Stokes equations. Even though the pressure field can vary in time and space, but no mechanism for sound generation is included in the above formulation. One can always consider the compressible Navier–Stokes equations at the limit of low Mach numbers to account for pressure fluctuations and sound generation. However, the present numerical techniques for the solution of compressible flows become very inefficient as the Mach number approaches zero.

To overcome this problem Hardin and Pope [4] suggested a rather simple and practical acoustic/viscous splitting technique that enables one to solve the time-dependent incompressible Navier–Stokes equations for the velocity and pressure fields. Then, using the time averaged pressure, they introduced a hydrodynamic density fluctuation correction term that is the source of sound generation in the inviscid fluctuating acoustic equations. The variable density correction accounts for density variations safely neglected in computing incompressible pressure field. These density fluctuations, which take place in the 'incompressible' flow, can be shown to be quite large compared to acoustic density fluctuations [4]. Details of this technique are explained below.

The Hardin–Pope splitting method introduces the following flow variables decomposition $u = U + u'$, $v = V + v'$, $p = P + p'$, and $\rho = \rho_0 + \rho_1 + \rho'$. Here, capital letters indicate incompressible viscous flow variables and primed variables indicate their inviscid acoustic fluctuating components. The ambient hydrostatic density is denoted by ρ_0 and the hydrodynamic density fluctuation correction $\rho_1 = \rho_1(x,t)$ is defined as

$$\rho_1 = (P - \bar{P})/c_0^2 \tag{1}$$

where $c_0 = (\gamma p_0/\rho_0)^{1/2}$ is the speed of sound in the far-field ambient fluid and the time averaged pressure for stationary flow fields is defined as

$$\bar{P} = \lim_{T\to\infty} \frac{1}{T} \int_0^T P \, \mathrm{d}t$$

The incompressible flow field variables U, V, and P are known through the numerical solution of the time-dependent incompressible Navier–Stokes equations or from an analytic solution.

The equations governing the acoustic field induced by low speed flows are obtained by utilizing the above decomposition in the compressible mass and momentum equations and then subtracting the incompressible Navier–Stokes equations from them, see Reference [4] for complete details. The acoustic field equations are given in a compact form as

$$\frac{\partial \hat{q}}{\partial t} + \frac{\partial \hat{f}}{\partial x} + \frac{\partial \hat{g}}{\partial y} = \hat{h} \tag{2}$$

where

$$\hat{q} = \begin{pmatrix} \rho' \\ \rho u' + \rho' U \\ \rho v' + \rho' V \end{pmatrix}, \quad \hat{f} = \begin{pmatrix} \rho u' + \rho' U \\ \rho(2Uu' + u'^2) + \rho' U^2 + p' \\ \rho(Vu' + Uv' + u'v') + \rho' UV \end{pmatrix},$$

$$\hat{g} = \begin{pmatrix} \rho v' + \rho' V \\ \rho(Vu' + Uv' + u'v') + \rho' UV \\ \rho(2Vu' + v'^2) + \rho' V^2 + p' \end{pmatrix}$$

$$\hat{h} = -\begin{pmatrix} \partial/\partial t(\rho_1) + \partial/\partial x(\rho_1 U) + \partial/\partial y(\rho_1 V) \\ \partial/\partial t(\rho_1 U) + \partial/\partial x(\rho_1 U^2) + \partial/\partial y(\rho_1 UV) \\ \partial/\partial t(\rho_1 V) + \partial/\partial x(\rho_1 UV) + \partial/\partial y(\rho_1 V^2) \end{pmatrix}$$

In these equations, the acoustic variables are the acoustic density ρ' normalized by the free stream density ρ_0, the acoustic velocities u' and v' normalized by the far-field speed of sound c_0, and the acoustic pressure p' normalized by $\rho_0 c_0^2$. The fluctuating energy equation can be used to obtain a relation for the acoustic pressure in terms of density; however since the acoustic field is considered to be isentropic, then the pressure and density are related through an isentropic relation, $p/p_{\mathrm{ref}} = (\rho/\rho_{\mathrm{ref}})^r$, and the use of the fluctuating energy equation is redundant. The non-dimensional form of this relation determines the acoustic pressure as

$$p' = (\rho^\gamma/\gamma) - P \tag{3}$$

These equations can be rewritten in a primitive variable form as follows:

$$\frac{\partial q}{\partial t} + A \frac{\partial q}{\partial x} + B \frac{\partial q}{\partial y} = S \tag{4}$$

where A and B are the coefficient matrices, S is the source term matrix and q is the primitive variable vector of the acoustic fluctuations $q = (\rho', u', v')^{\mathrm{T}}$. The coefficient and the source term matrices for a Cartesian co-ordinate system are given in Appendix A.

3. LINEARIZED ACOUSTIC FIELD EQUATIONS

The acoustic field equations are non-linear and this enables them to capture such non-linear phenomena as non-linear wave interactions and wave steepening. However this non-linearity makes their numerical solution very time consuming, especially for complex three-dimensional geometries. If a reasonable linearization of the equations proves feasible, simpler numerical schemes with less stringent computational requirements can be designed for their solution. Furthermore, extension of these schemes to three-dimensional problems involving complex geometries can be realized on small workstations and leading edge personal computers. The idea of a linearization is strongly supported by the fact that non-linearity effects are very mild in the case of the generation and propagation of the acoustic waves by low Mach number flows. The non-linear phenomena such as wave steepening are absent or very weak if the flow region is not confined and there are no vibrating walls. In many low Mach number flows unsteady vortex dynamic and/or shear layers are the main source of noise. The acoustic source in these flows is similar in nature to a quadrupole source and therefore it is reasonable to linearize the acoustic field equations.

In the present study the spinning vortex pair with its quadrupole acoustic source is used to evaluate non-linearity effects in an unconfined region. The results of this study can be extended to low Mach number external flows containing vortices and shear layers in absence of vibrating walls.

It is well known that acoustic fluctuations are much smaller than their incompressible flow field counterparts:

$$\begin{aligned} v_i' &\ll V_i \\ \rho' &\ll \rho_0 + \rho_1 \end{aligned} \tag{5}$$

Also pressure changes due to minor density changes can be neglected in evaluating the speed of sound and a uniform speed of sound can be considered throughout the computational domain. Therefore, the following approximate values may be used to linearize acoustic field equations:

$$\begin{aligned} v_i &\approx V_i \\ \rho &\approx \rho_0 + \rho_1 \\ c &\approx c_0 \end{aligned} \tag{6}$$

The linearized primitive variable form of the acoustic field equations, given by Equation (4), may be rewritten as

$$\begin{aligned} \frac{\partial \rho'}{\partial t} + V \cdot \nabla \rho' + \rho_0 \nabla \cdot v' &= -\left(\frac{\partial \rho_1}{\partial t} + v \cdot \nabla \rho_1 \right) \\ \frac{\partial v'}{\partial t} + V \cdot \nabla v' + \frac{\nabla p'}{\rho_0} &= -\left[\bar{\rho} \frac{\partial V}{\partial t} + (\bar{\rho} V + v') \cdot \nabla V \right] \\ \frac{\partial p'}{\partial t} + V \cdot \nabla p' + \rho_0 c_0^2 \nabla \cdot v' &= 0 \end{aligned} \tag{7}$$

The numerical solutions of the linearized and non-linear acoustic field equations are discussed in the following section.

4. NUMERICAL CONSIDERATIONS

The acoustic field equations, proposed by Hardin and Pope, have been solved numerically using classical CFD schemes in References [5–8]. In the present study optimized high order DRP schemes are utilized.

Time marching is carried out by an explicit fourth-order accurate DRP scheme [9]. In comparison with the usual fourth-order Runge–Kutta schemes the fourth-order DRP scheme requires more space to store residual terms at four different time steps. However, one-dimensional case studies indicate that the usual fourth-order Runge–Kutta schemes require more computing time due to computation of four different residual terms at every time step [11].

Low order spatial differencing adds too much numerical error to the difference equations and cannot be used for aeroacoustic predictions with a reasonable number of points per wavelength of the shortest wave desired to be resolved. High bandwidth schemes are required for an accurate solution of the aeroacoustic problems [10]. The bandwidth of a discrete operator refers to the range of wave numbers resolved by the operator. One strategy to create operators that are useful over a larger bandwidth is to reduce the order property below the maximum order possible for a given stencil. The reduced order provides additional degrees of freedom that can be used to optimize the operator. The stencil and, thus, the computational effort remains identical to the original operator.

Suppose that an $M+N+1$ point finite difference stencil is used to approximate the first derivative $\partial f/\partial x$ at the point x of a grid with spacing Δx, i.e.

$$\frac{\partial f}{\partial x}(x) \approx \frac{1}{\Delta x} \sum_{j=-M}^{N} a_j f(x + j\Delta x) \tag{8}$$

The effective numerical wave number of the finite difference scheme can be calculated by the application of the Fourier transformation on both sides of Equation (8), as

$$\bar{\alpha} = \frac{-i}{\Delta x} \sum_{j=-M}^{N} a_j e^{ij\alpha\Delta x} \tag{9}$$

In a DRP scheme, coefficients a_j are determined so that Equation (9) is accurate to the order of $\Delta x^{(M+N-2)}$ through Taylor series expansion, and then the remaining unknowns are chosen in a way that $\bar{\alpha}$ is a close approximation of α over a wide band of wave numbers. The numerical values of a_j are tabulated in Reference [10].

In this study, fourth-order accurate optimized DRP schemes are used for space dicretization of the acoustic field equations. Spatial differencing can be achieved by upwind or central differencing schemes. Upwinding is based on the eigenvalue sign of the coefficient matrices. The coefficient matrices A and B are diagonalized as follows:

$$A^{\pm} = X_A \Lambda_A^{\pm} X_A^{-1}, \quad B^{\pm} = X_B \Lambda_B^{\pm} X_B^{-1} \tag{10}$$

where Λ_A and Λ_B are diagonal matrices containing the eigenvalues of A and B, X_A and X_B are the left eigenvector, and X_A^{-1} and X_B^{-1} are the right eigenvector matrices of A and B, respectively. The residual term of the time marching

$$\frac{\partial q}{\partial t} = R = S - (Aq_x + Bq_y) \tag{11}$$

is computed as

$$R = S - [(A^+ q_x^- + A^- q_x^+) + (B^+ q_y^- + B^- q_y^+)] \tag{12}$$

where q^+ and q^- are calculated using forward and backward upwind difference operators, respectively.

Application of high order central differencing schemes to linearized equations can reduce the computational effort by eliminating the requirement of computing the eigenvalues and corresponding matrices. Equation (11) can be used directly to evaluate the residual terms. The disadvantage of the central difference schemes is their inherent dependency in time and space discritization. Selective artificial damping terms must be added to obtain a stable scheme. An appropriate damping term is given by [10]

$$-\frac{v_a}{\Delta x_i^2} \sum_{j=-3}^{3} d_j e^{-ij\alpha\Delta x_i} \tag{13}$$

where $[v_a/\Delta x_i^2]$ is the damping coefficient and Δx_i is the grid spacing in ith direction.

Upwind and central differencing schemes are applied to the solution of the non-linear acoustic field equations, however, due to the simplicity of the linearized acoustic field equations only the central differencing scheme is used for their solution. Results are discussed after a brief review of the boundary conditions.

5. BOUNDARY CONDITIONS

A computational domain is inevitably finite in size. Therefore, appropriate boundary conditions are required at the domain's computational boundaries. These boundary conditions allow the acoustic and flow disturbances to leave the computational domain with minimal reflection. Acoustic radiation boundary conditions of Tam and Webb [9] are applied at the far-field boundaries and the following set of differential equations are used to find the acoustic fluctuations at boundaries:

$$\frac{1}{\tilde{V}(r,\theta)} \left(\frac{\partial}{\partial t} + \frac{\partial}{\partial r} + \frac{1}{2r} \right) q_b = 0 \tag{14}$$

where $q_b = (\rho' + \rho_1, u', v')^T$, $\tilde{V}(r,\theta) = U\cos\theta + V\sin\theta$ and (r,θ) are polar co-ordinates centred near the middle of the computation domain. Equation (14) is solved with an explicit scheme. The time derivative is discretized using a first-order time accurate operator.

6. RESULTS AND DISCUSSION

In order to assess the effect of the non-linear terms in the acoustic field equations and to evaluate the performance of the proposed high order schemes, the sound field generated by a co-rotating vortex pair is investigated. This model problem is chosen because there exist analytical solutions for the flow and the acoustic field generated by a pair of point vortices [12]. The existence of an exact flow field solution facilitates the evaluation of the numerical schemes utilized for the solution of the acoustic field equations without suffering any possible uncertainties imposed by numerical solution of the incompressible flow field. Others have used this same problem to assess the accuracy of the numerical schemes proposed for solving the governing equations in both original and primitive variable forms [6–8].

An acoustic field is generated by the inherent unsteadiness of the incompressible flow field of a spinning vortex pair. The two-point vortices, separated by a distance $2r_0$, rotate around each other along a circular path of radius r_0 with a circulation intensity of Γ, a period of $T = 8\pi^2 r_0^2/\Gamma$, a rotating speed of $\omega = \Gamma/4\pi r_0^2$, and a rotating Mach number of $M_r = \Gamma/4\pi r_0 c_0$, see Figure 1.

Müller and Obermeier [12] used the method of matched asymptotic expansions for theoretical analysis of the spinning vortices. In their analysis, the incompressible flow is considered as the inner solution and the perturbed compressible flow field as the outer solution. These solutions are matched in an intermediate region in such a way as to give an asymptotically valid solution. Following this analysis, the hydrodynamic velocity and pressure and the acoustic

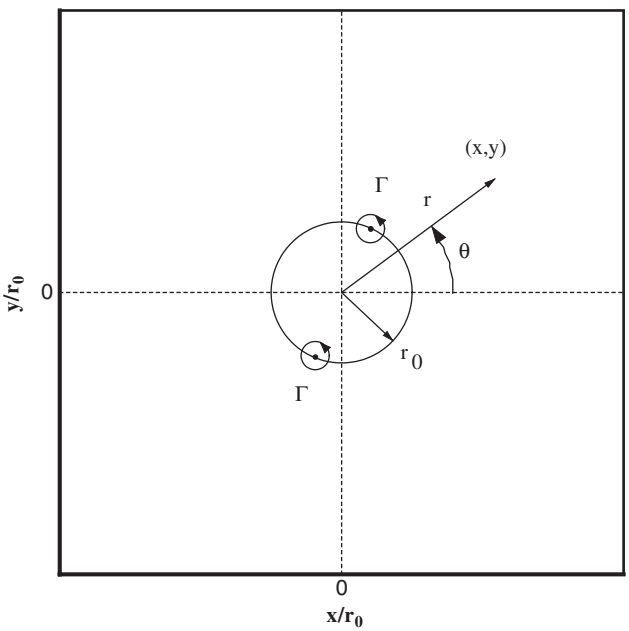

Figure 1. Schematic configuration of corotating vortices.

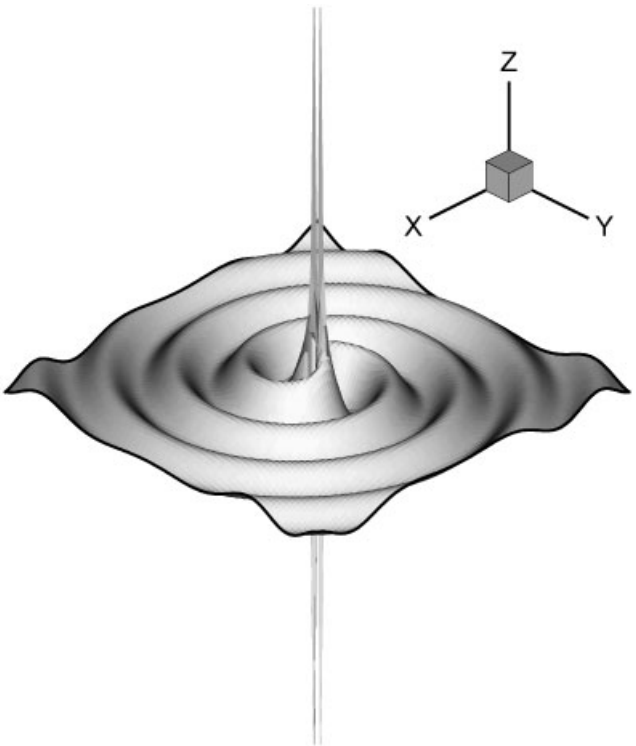

Figure 2. 3-D view of analytic solution for acoustic pressure.

pressure fluctuations are obtained as

$$U - \mathrm{i}V = \frac{\Gamma}{\mathrm{i}\pi}\frac{z}{z^2 - b^2}$$

$$P = P_0 + \rho_0 \frac{\Gamma\omega}{\pi}\Re\left(\frac{b^2}{z^2 - b^2}\right) - \frac{1}{2}\rho_0(U^2 + V^2) \tag{15}$$

$$p' = \frac{\rho_0\Gamma^4}{64\pi^3 r_0^4 c_0^2}[J_2(kr)\cos(2(\omega t - \theta)) - Y_2(kr)\sin(2(\omega t - \theta))]$$

where $z = x + \mathrm{i}y = r\mathrm{e}^{\mathrm{i}\theta}$, $b = r_0\mathrm{e}^{\mathrm{i}\theta}$, $\Re$ denotes the real part operator, $k = 2\omega/c_0$, and $J_2(z)$ and $Y_2(z)$ are the second-order Bessel functions of the first and second kind, respectively. Figure 2 shows a 3-D graphical view of the acoustic pressure fluctuations when $\Gamma = 2\pi/10$ and $M_\mathrm{r} = 0.1$.

At the mid-distance between the vortices, the acoustic pressure becomes singular and very close to the vortex centres the hydrodynamic velocity and pressure have large gradients. To avoid numerical singularity at the centre of the vortices a vortex core model is required [6]. The Scully [13] vortex model as described below is used in this study. In this model the

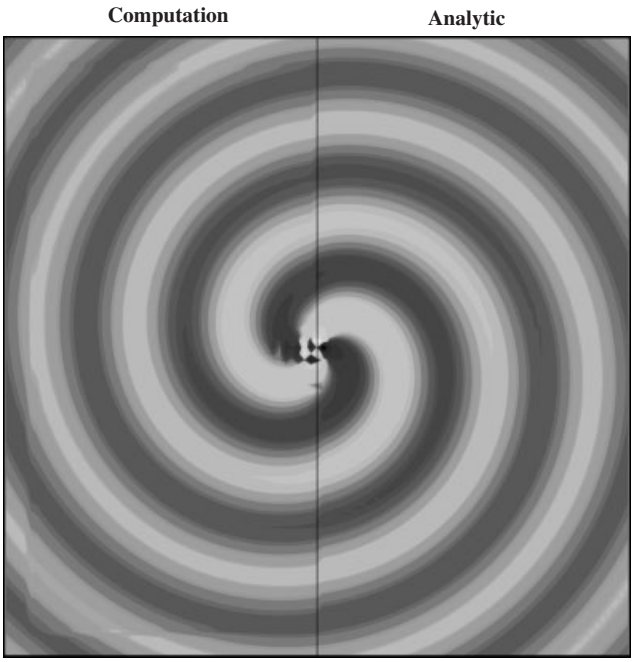

Figure 3. Comparison of the analytic and computed acoustic pressure fields for $\Gamma = 2\pi/10$ and $M_r = 0.1$.

tangential velocity component is approximated as

$$V_\theta = \frac{\Gamma r}{2\pi(r_c^2 + r^2)} \tag{16}$$

where V_θ is the tangential velocity, r is the radial distance from the vortex centre, and r_c is the core radius.

A square computational domain centred at the origin of the co-ordinate system with sides equal to $300r_0$ and uniform square grids is considered. Zero initial values are used for all acoustic fluctuations. The computations are continued until temporal periodicity is obtained.

Based on the exact solution given by Equation (15) the distance between the vortex pair, r_0, and the circulation intensity, Γ, for a given value of speed of sound are the only parameters determining the frequency, amplitude and spatial attenuation of the solution. In another word the circulation intensity and the rotating Mach number determine the grid and time step resolutions for an accurate and stable solution. However, the overall dynamics of the problem is not affected by changing any of these parameters. Therefore, solutions are obtained and presented only for $\Gamma = 2\pi/10$ and $M_r = 0.1$ to avoid an extensive computational effort.

The non-linear acoustic field equations are solved by the upwind-biased scheme and the results are compared with the exact solution. Figure 3 shows a qualitative agreement between numerical and analytical acoustic pressure contours.

Figure 4 shows a more quantitative comparison between numerical and analytical solutions. The acoustic pressure distribution along horizontal axis is extracted and depicted in this figure. Although relatively coarse grid with $\Delta x/r_0 = 4$ and moderate time step with $\Delta t = 0.01$ are used

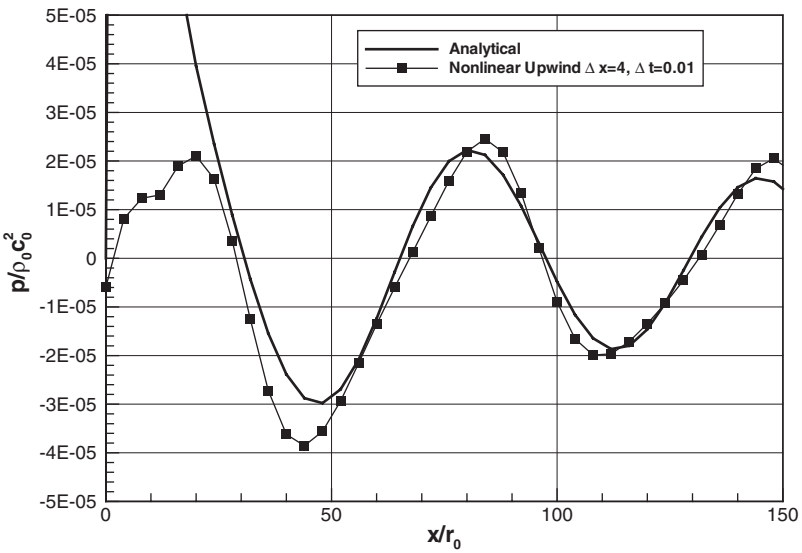

Figure 4. Comparison of the analytical and computed results along x-axis for $\Gamma = 2\pi/10$ and $M_r = 0.1$ with non-linear acoustic field equations.

in this simulation, dissipation and dispersion errors are bounded to reasonable amounts except near the centre of the vortices where acoustic pressure becomes singular. This reveals the ability of the acoustic/viscous splitting technique combined with the high order DRP scheme in predicting the sound generation and propagation by quadruple sources.

The linearized acoustic field equations can also be solved using a high order central DRP scheme. To achieve a stable solution with the central difference schemes an appropriate damping factor causing the least possible artificial damping is required. An appropriate damping factor is obtained by simulation of the linearized equations and comparison of the results with the exact analytical solution. To be consistent the same damping factor is used for non-linear as well as linearized simulations. To this end, a high order central DRP scheme with different damping factors ranging from 0.125 to 0.5 is used to solve the linearized acoustic field equations. Figure 5 shows the extracted values of the computed results along the horizontal axis and compares them with the analytical results. Based on these results a damping factor of 0.25 is chosen for the rest of the computations.

To investigate effects of linearizing the acoustic field equations, non-linear simulation results are compared with linearized approximations in Figure 6. Both upwind and central DRP schemes for non-linear simulations and the central DRP scheme for linear simulations are used in this study. It shows that non-linear and linearized results are nearly indistinguishable and their difference is even less than the difference between non-linear results and analytical solution. The main advantage of the linearization proposed in this study lies in a considerable simplification of the computational procedure and consequently results in a valuable time saving. Table I compares total CPU time needed for 100 000 iterations of the linearized and non-linear simulations. All of the computations were carried out on a 633 MHz Intel Pentium III

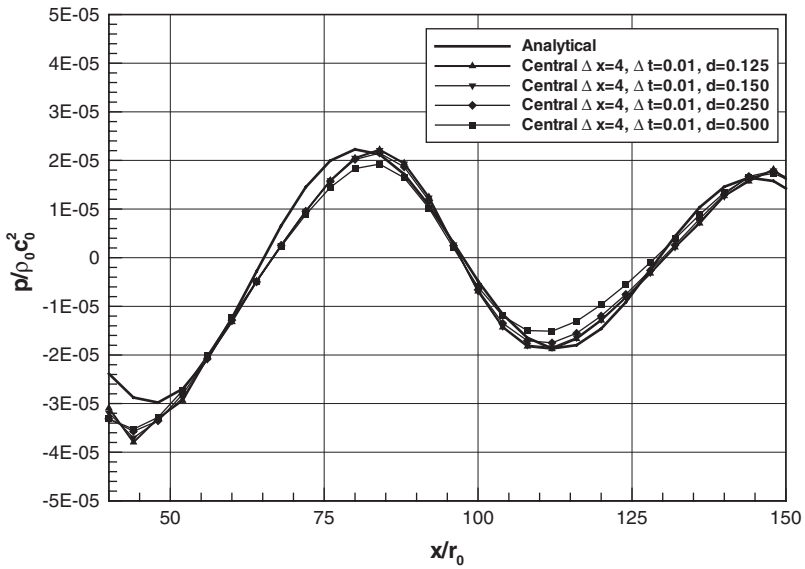

Figure 5. Comparison of the analytical and computed results along x-axis for $\Gamma = 2\pi/10$ and $M_r = 0.1$ with different damping factors using linearized acoustic field equations.

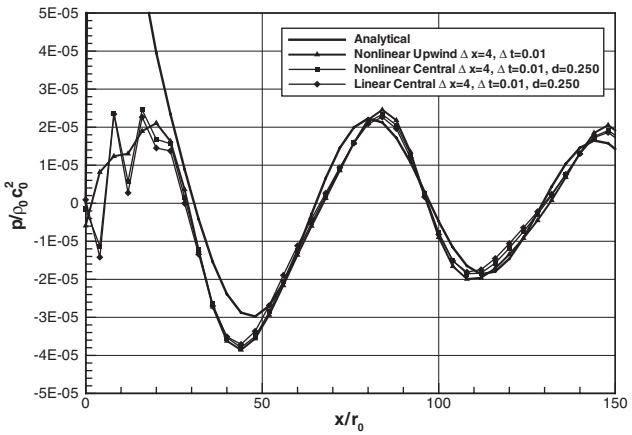

Figure 6. Comparison of the analytical and computed results along x-axis for $\Gamma = 2\pi/10$ and $M_r = 0.1$ with linearized and non-linear equations.

with 256 MB of RAM. It is shown that non-linear calculations take about 160% more time than the linearized calculations for the same number of iterations.

A grid resolution study is also carried out. In Figure 7 extracted values of the analytical and linearized solutions along the horizontal axis obtained with two different grid spacings are compared. Central DRP schemes with damping terms were used in both simulations. Good agreement is observed except near the centre of the vortices where the acoustic pressure becomes singular. It is shown that using a coarse grid spacing of $\Delta x/r_0 = 4$, with about 11

Table I. CPU time comparsion of non-linear and linearized schemes (100 000 iterations).

Case	Solver	$\Delta x/r_0$	$\Delta y/r_0$	Δt	Damping factor	CPU time (s)
1	Non-linear	4	4	0.01	0.25	13 078
2	Linearized	4	4	0.01	0.25	4988
3	Non-linear	8	8	0.01	0.25	3272
4	Linearized	8	8	0.01	0.25	1248

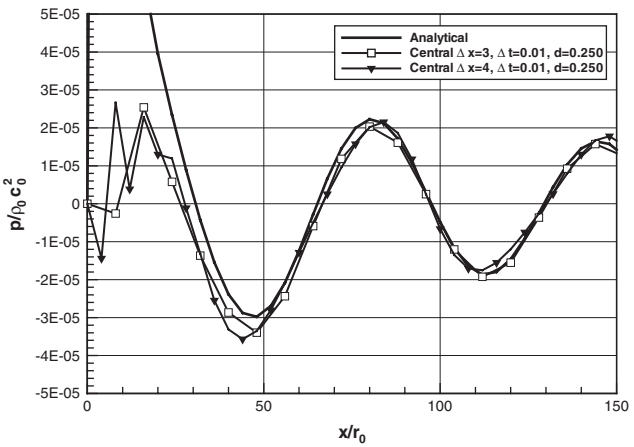

Figure 7. Comparison of the analytical and computed results along x-axis for $\Gamma = 2\pi/10$ and $M_r = 0.1$ with different mesh spacings using linearized equations.

points per wavelength (PPW), provides as good a result as those obtained for the case of $\Delta x/r_0 = 3$, with about 15 PPW, except near the centre of the vortices. Hence grid independency is achieved with $\Delta x/r_0 = 4$. It is noticeable that Lee and Koo [6] have reported using a minimum of 25 PPW with a MacCormack predictor–corrector scheme to obtain a comparable level of accuracy. Therefore, the DRP scheme can provide more than 50% savings in the spatial resolution compared with lower order schemes.

The effect of time step on the solution of the linearized equations is investigated last. The results obtained by two different time steps are compared with analytical solution in Figure 8. Both solutions are extracted at the same time using $\Delta x/r_0 = 3$. The solution computed with the larger time step shows a notable deviation from the analytical solution, but the solution computed by smaller time step picks up the analytical solution a wavelength away from the source. Using time steps larger than 0.075, which appears to be the stability limit of the time integration, gives rise to unstable solutions. The accuracy of the solution is not practically increased with decreasing time step below 0.01 as the result obtained using this time step nearly falls on the analytical solution at the far field.

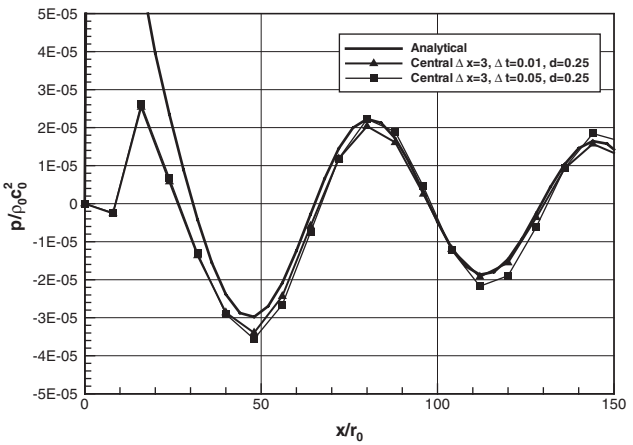

Figure 8. Comparison of the analytical and computed results along x-axis for $\Gamma = 2\pi/10$ and $M_r = 0.1$ with different time steps using linearized equations.

7. CONCLUSION

An acoustic/viscous splitting technique has been applied to the incompressible Navier–Stokes equations to obtain an acoustic field equation governing the generation and propagation of sound in low Mach number flow fields. Next an optimized high order DRP scheme is utilized to solve the acoustic field equations for the solution of the sound generated by a spinning vortex pair. The results show that the application of this method provides a good solution even on relatively coarse grids. Finally, the acoustic field equations are linearized and then solved by high order DRP schemes. It is observed that the error introduced into simulations by this approximation is even less than the numerical error in simulating non-linear equations. The prime advantage of this linearization is a substantial simplification of the solution procedure and consequently notable timesavings. It is observed that non-linear calculations take about 160% more time than the linearized calculations for the same number of iterations. This is a promising timesaving approach for the simulation of three-dimensional acoustic fields generated by low Mach number flows.

APPENDIX A

The coefficient and the source term matrices in the cartesian co-ordinates are given by

$$A = \begin{bmatrix} u & \rho & 0 \\ c^2/\rho & u & 0 \\ 0 & 0 & u \end{bmatrix}, \quad B = \begin{bmatrix} v & 0 & \rho \\ 0 & v & 0 \\ c^2/\rho & 0 & v \end{bmatrix},$$

$$S = -\begin{bmatrix} \dfrac{\partial \rho_1}{\partial t} + u\dfrac{\partial \rho_1}{\partial x} + v\dfrac{\partial \rho_1}{\partial y} \\ \bar{\rho}\dfrac{\partial U}{\partial t} + (\bar{\rho}U + u')\dfrac{\partial U}{\partial x} + (\bar{\rho}V + v')\dfrac{\partial U}{\partial y} \\ \bar{\rho}\dfrac{\partial V}{\partial t} + (\bar{\rho}U + u')\dfrac{\partial V}{\partial x} + (\bar{\rho}V + v')\dfrac{\partial V}{\partial y} \end{bmatrix}$$

where $\bar{\rho} = (\rho_1 + \rho')/\rho$.

REFERENCES

1. Mitchell BE, Lele SK, Moin P. Direct computation of sound from a compressible co-rotating vortex pair. *Journal of Fluid Mechanics* 1995; **285**:58–78.
2. Colonius T, Lele SK, Moin P. Scattering of sound waves by compressible vortex. *AIAA Paper* 91-0494, January 1991.
3. Lele SK. Direct numerical simulation of compressible free shear flows. *AIAA Paper* 89-0374, January 1989.
4. Hardin JC, Pope SD. An acoustic/viscous splitting technique for computational aeroacoustics. *Theoretical and Computational Fluid Dynamics* 1994; **6**(5–6):334–340.
5. Hardin JC, Pope SD. Sound generation by flow over a two-dimensional cavity. *AIAA Journal* 1995; **33**(3): 407–412.
6. Lee DJ, Koo SO. Numerical study of sound generation due to a spinning vortex pair. *AIAA Journal* 1995; **33**(1):20–26.
7. Ekaterinaris JA. An upwind scheme for the computation of acoustic fields generated by incompressible flow. *AIAA Journal* 1997; **35**(9):1448–1455.
8. Ekaterinaris JA. New formulation of Hardin–Pope equations for aeroacoustics. *AIAA Journal* 1999; **37**(9): 1033–1039.
9. Tam CKW, Webb JC. Dispersion–relation–preserving schemes for computational aeroacoustics. *Journal Computational Physics* 1993; **107**(2):262–281.
10. Tam CKW. Computational aeroacoustics: issues and methods. *AIAA Journal* 1995; **33**(10):1788–1796.
11. Ebrahimi M. Computational aeroacoustics analysis and its application to cabin noise prediction. *Ph.D. dissertation*, Sharif University of Technology, 2002.
12. Müller E-A, Obermeier F. The spinning vortices as a source of sound. *Journal of Fluid Mechanics* 1967; **85**(4):685–691.
13. Scully MP. *Computation of Helicopter Rotor Wake Geometry and its Influence on Rotor Harmonic Air Loads*. Massachusetts Institute of Technology, Pub. ARSL TR 178-1: Cambridge, MA, March 1975.

